Cancer Research

Multiregion Whole-Exome Sequencing Uncovers the Genetic Evolution and Mutational Heterogeneity of Early-Stage Metastatic Melanoma

Katja Harbst[1], Martin Lauss[1], Helena Cirenajwis[1], Karolin Isaksson[2], Frida Rosengren[1], Therese Törngren[1], Anders Kvist[1], Maria C. Johansson[1], Johan Vallon-Christersson[1], Bo Baldetorp[1], Åke Borg[1], Håkan Olsson[1,3], Christian Ingvar[2,4], Ana Carneiro[1,3], and Göran Jönsson[1]

Abstract

Cancer genome sequencing has shed light on the underlying genetic aberrations that drive tumorigenesis. However, current sequencing-based strategies, which focus on a single tumor biopsy, fail to take into account intratumoral heterogeneity. To address this challenge and elucidate the evolutionary history of melanoma, we performed whole-exome and transcriptome sequencing of 41 multiple melanoma biopsies from eight individual tumors. This approach revealed heterogeneous somatic mutations in the range of 3%–38% in individual tumors. Known mutations in melanoma drivers BRAF and NRAS were always ubiquitous events. Using RNA sequencing, we found that the majority of mutations were not expressed or were expressed at very low levels, and preferential expression of a particular mutated allele did not occur frequently. In addition, we found that the proportion of ultraviolet B (UVB) radiation-induced C>T transitions differed significantly ($P < 0.001$) between early and late mutation acquisition, suggesting that different mutational processes operate during the evolution of metastatic melanoma. Finally, clinical history reports revealed that patients harboring a high degree of mutational heterogeneity were associated with more aggressive disease progression. In conclusion, our multiregion tumor-sequencing approach highlights the genetic evolution and non-UVB mutational signatures associated with melanoma development and progression, and may provide a more comprehensive perspective of patient outcome. *Cancer Res; 76(16); 4765–74. ©2016 AACR.*

Introduction

Intratumor heterogeneity (ITH) has recently been thoroughly examined in cancer using whole-exome sequencing (WES) of multiple regions of a sample (1–8). ITH could have major implications for clinical strategies concerning biopsy representation of the tumor, clonality of alterations in targetable genes, and drug resistance. In renal cell carcinoma, substantial ITH was demonstrated with up to 70% of mutations occurring in a heterogeneous pattern across spatially separated regions in individual tumors. Several known cancer gene mutations were confined to distinct regions (2). Lung adenocarcinomas have also been analyzed using a similar multiregion approach (3, 4). Although lung adenocarcinomas are also characterized by ITH, 76% of all mutations were identified in all tumor regions. Furthermore, somatic mutations acquired during the progression of the tumors tended to be less smoking induced and instead had evidence of being acquired through upregulation of APOBEC cytidine deaminases (9). Other studies using multiregion sequencing of tumors revealed different extent of heterogeneity depending on the tumor type, for example, close to 100% heterogeneous genetic alterations in multifocal prostate cancer (6, 7), 55% in esophageal adenocarcinoma (8), and 49% in ovarian cancer (5). Overall, these data point to the fact that single-biopsy strategies may be inadequate to inform on mutation status and may lead to significant molecular information being missed.

We recently found evidence of intrapatient tumor heterogeneity, using targeted gene sequencing and gene expression microarray analysis, in treatment-naïve metastatic melanoma patients (10). Furthermore, individual metastases have been shown to be founded by multiple cell populations in the primary melanoma (11) highlighting the complexity of metastatic progression. Although few treatments have been available in metastatic melanoma, the recent development of inhibitors targeting BRAF and MEK changed the clinical outcome of patients with metastatic disease (12). However, in most cases,

[1]Division of Oncology and Pathology, Department of Clinical Sciences, Lund University, Lund, Sweden. [2]Department of Surgery, Skåne University Hospital, Lund, Sweden. [3]Department of Oncology, Skåne University Hospital, Lund, Sweden. [4]Division of Surgery, Department of Clinical Sciences, Lund University, Lund, Sweden.

Note: Supplementary data for this article are available at Cancer Research Online (http://cancerres.aacrjournals.org/).

K. Harbst, M. Lauss, A. Carneiro, and G. Jönsson contributed equally to this article.

Corresponding Author: Göran Jönsson, Division of Oncology and Pathology, Department of Clinical Sciences, Lund University, Lund, Sweden. Phone: 464-6222-0383; Fax: 464-614-7327; E-mail: goran_b.jonsson@med.lu.se

doi: 10.1158/0008-5472.CAN-15-3476

Table 1. Clinical features of patients included in the study

Patient	Disease state at surgery	Treatment (after surgery)	Overall survival (months from surgery)	Patient status	Number of samples
Mm1641	Lymph node and lung metastases	BRAF inhibitor	6	Dead of disease	7
Mm1702	Lymph node and lung metastases	Dacarbazine	5	Dead of disease	3
Mm1765	Primary melanoma	No treatment	NA	NA	4
Mm1767	Lymph node metastasis	No treatment	12	Alive	4
Mm1772	Lymph node and skeletal metastases	Ipilimumab, Pembrolizumab	11	Alive	4
Mm1837[a]	Primary melanoma	Nivolumab	6	Dead of disease	3
Mm1749[b]	In-transit metastasis	Ipilumumab	48	Dead of disease	9
Mm1742[c]	Lymph-node	Temozolomide, Pembrolizumab, Ipilimumab	26	Dead of disease	3

[a]This patient died within one month of stage IV diagnosis.
[b]Nine in-transit metastases were obtained from this patient.
[c]This patient was treated with temozolomide during surgery.

the success is limited by the development of resistance in the majority of patients within 6–9 months from treatment initiation. Several groups have studied whether genetic heterogeneity can explain therapy resistance (4, 13, 14) and further highlighting the complex heterogeneity of therapy resistance, it has been shown that different mechanisms of resistance occur simultaneously in a single melanoma patient (15). Whether these genetic lesions exist in small subclones prior to treatment initiation still remains unclear.

To address these challenges, we applied multiregion DNA and RNA sequencing to melanoma tumors from eight patients. Our findings shed light on the extent of ITH in treatment-naïve melanoma, help to separate early from late genetic events, and decipher mutational spectra occurring during the course of early metastatic disease.

Patients and Methods

Patient selection

Patients ($n = 8$; Table 1) were selected for the study by a surgeon or oncologist based on the size of the tumor to allow for sampling of each quadrant of the tumor (see Supplementary Information). The biopsies were taken at surgery and immediately stored at −80°C (see Supplementary Fig. S1 for study workflow). We collected frozen tissue from multiple spatially separated tumor regions (Supplementary Table S1). Six patients had metastatic disease at the time of surgery, and for two patients (Mm1765, Mm1837) the primary melanoma was biopsied. In one case (Mm1742), the inguinal metastasis was removed during temozolomide treatment due to local progress and should be considered separately in all subsequent analyses. All other cases were untreated at the time of surgical removal of tumor.

For patient Mm1702, only three different core-needle biopsies were analyzed. Blood samples were available from all patients except for Mm1837, for whom normal skin was used as matched normal control. All patients consented and the study was approved by the Regional Ethical Committee (Dnr. 101/2013).

Nucleic acid extraction

DNA and RNA were extracted from tumor and normal skin using AllPrep DNA/RNA Mini Kit (Qiagen). DNA was extracted from blood using QIAamp DNA Blood Mini Kit (Qiagen).

Whole-exome sequencing

Tumor and matched normal DNA samples were subjected to library preparation. All sample libraries except Mm1641 were prepared according to SureSelect Target Enrichment System for Illumina Paired-End Sequencing Library Protocol (Agilent Technologies), using Clinical Research Exome (CRE) capture oligo panel. For Mm1641, libraries were prepared using the following three platforms: SureSelect All Exon V5+UTR (Agilent Technologies); TruSeqProtocol with TruSeq Exome Enrichment (Illumina); and Nextera Rapid Capture Protocol with Expanded Exome (Illumina). All biopsies were sequenced with a physical coverage of at least 120× with the exception of Mm1641 (coverage 220×). Libraries were sequenced on a HiSeq 2500 using normal or rapid run mode.

WES data analysis

Reads were mapped to the human reference genome (hg19) with decoy using Novoalign (Novocraft Technologies). Postalignment processing is described in the Supplementary Information. For variant calling, MuTect (16) and VarScan (17) were used, and consensus calls between the two in the coding parts of the genes by Annovar annotation (18) were retained (see Supplementary Information). Copy number log ratios of sequenced exons were generated from bam files of tumor–normal pairs using CONTRA 2.03, with default parameters (19). Exons with insufficient coverage in the normal sample were removed. Copy number data were segmented using GLAD (20).

Phylogenetic and subclonality analysis

Phylogenetic trees of single-nucleotide variation (SNV) data were generated using the maximum parsimony method. ABSOLUTE (21) was used for the identification of cancer cell fractions of SNVs with support from segmented copy number data and FACS ploidy analysis (for details see Supplementary Information).

Gene expression analysis

Gene expression levels of multiregion samples were assayed using the Illumina HT12 microarray platform according to the manufacturer's instructions at the Swegene Center for Integrative Biology at Lund University. Data analysis included integration of the multiregion samples with a reference set of 214 melanomas (22) and subtype classification (Supplementary Information).

Allele-specific expression at mutation sites

RNA-seq was performed using the Illumina NextSeq for the multiregion samples largely as described by Saal and colleagues (23) but using Illumina TruSeq Stranded mRNA Library Prep Kit and NextSeq500. Mm1641:R1 and Mm1749:R6 were omitted due to lack of input mRNA. For details on RNA-seq

and allele-specific expression analysis see Supplementary Information.

Results

Analysis of intratumor heterogeneity in melanoma tumors

WES was performed on 41 tumor samples obtained from eight patients with an average target depth of 120× per sample (220× for Mm1641). Overall, three samples were excluded due to high normal tissue admixture (see Supplementary Information). We called a mutation being present in a tumor if a nucleotide substitution was present in at least 10% of reads in at least one tumor region. We then determined the regional distribution of nonsynonymous mutations based on the WES data. We found on average 489 (range 45–814) nonsynonymous mutations per tumor whereof 13% (range 2.7%–37.8%) of the nonsynonymous somatic mutations were heterogeneous, that is, not detected across all sampled regions in the individual tumors (Fig. 1). Notably, mutational ITH was not obvious at the morphologic level, with uniform appearance of the tumor throughout its regions (Supplementary Fig. S2). In melanoma, three genes (*BRAF*, *NRAS*, and *NF1*), all key components of the MAPK pathway, are frequently mutated and overall demonstrate a mutually exclusive pattern (24). We found *BRAF* V600E mutation in two patients, three cases harbored *NRAS* Q61 mutation, one case had both *NRAS* Q61 and *NF1* mutation, and one case had both *KIT* and *NF1* mutation. *KIT* is rarely mutated in cutaneous melanoma; however, it is a known oncogenic driver in acral and mucosal melanoma (25). These mutations were present across the tumor regions at similar allele frequencies (Supplementary Table S1). The Mm1767 tumor, which did not receive treatment regimens prior to surgical removal, had the lowest degree of mutational heterogeneity with 546 nonsynonymous somatic mutations, of which only 2.7% were not detected in all spatially separated regions. Three patients (Mm1837, Mm1641, Mm1702) died of their disease within six months of the analyzed biopsy (Table 1). These had higher degree of mutational heterogeneity as compared with the other patients ($P = 0.03$, t test). Seven spatially separated regions from a lymph node metastasis from patient Mm1641 exhibited 14.2% mutational heterogeneity. At the time of surgery, the patient had an aggressive disease and developed lung metastases. The patient subsequently received BRAF inhibitor therapy; however, after six months on therapy, the patient had a progressive disease course. From Mm1702, three core-needle biopsies in a lymph node metastasis were analyzed and revealed 20.9% mutational heterogeneity. In addition, FACS ploidy analysis revealed one hypo- and one hyper-tetraploid subclone in all tumor regions (Supplementary Fig. S3; Supplementary Table S2). At the time of diagnosis the patient presented with distant metastases to the lungs and shortly thereafter the patient developed meningeal carcinomatosis. The third patient (Mm1837) had 45 somatic mutations, which exhibited 37.8% mutational heterogeneity. The patient was diagnosed with a large primary melanoma (Breslow thickness 18 mm) of a nondefined pathologic subtype that was MLANA negative, and developed an aggressive metastatic disease six months after initial diagnosis. Two patients are currently alive, of which, one received both ipilumumab and pembrolizumab. These two patients had the lowest degree of heterogeneous mutations (2.7% and 5.4%, respectively; Table 1). Although intriguing, larger series are required to determine the usage of ITH as a biomarker in melanoma.

Analysis of regional subclones and mapping melanoma tumor evolution by phylogenetic tree analysis

Next, we mapped driver genes from Catalogue of Somatic Mutations in Cancer (COSMIC) Cancer Gene Census list (26) to determine whether mutations in previously identified cancer driver genes were predominantly trunk or branch mutations within the phylogenetic tree. We found 129 mutations in cancer driver genes with 113 mutations (88%) being trunk mutations while only 16 (12%) were branch mutations (Fig. 2). Mutations in the melanoma driver genes, *BRAF*, *NRAS*, and *NF1*, were always present on the trunk consistent with the critical role of constitutive activation of the MAPK pathway in the majority of melanomas. Although the majority of driver mutations detected in these melanomas appear to be present in all spatially separated regions (Figs. 1, 2A, and B), we also observed parallel evolution of subclones within the melanoma. For example, Mm1641 harbored three distinct and spatially separated activating mutations in *PIK3CA* (encoding p.R38H, p.V344G, and p.H1047R). Furthermore, a *PIK3R1* (encoding p.Q384X) truncating mutation was detected as part of the dominant clone in a distinct region (R5) wild-type for the three different *PIK3CA* mutations. In addition, a mutation in the phosphatase domain of *PTEN* (p.K125E) was present at high allele frequencies in all regions except R1. This mutation alters a highly conserved amino acid residue and was predicted "probably damaging" by PolyPhen-2 with a score of 0.999. Importantly, R1 harbored the H1047R *PIK3CA* kinase domain mutation frequently found to be mutually exclusive to *PTEN* mutations (27). The R7 region demonstrated the highest degree of subclonality that presumably includes the clones from R5 and R1 due to subclonal presence of mutations in *PIK3CA* (p.H1047R), *PTEN*, and *PIK3R1* (Fig. 2C and Supplementary Figs. S4–S8). Overall, parallel evolution converging on distinct genes in the same pathway indicates a strong selection for aberrations in these genes in the progression of melanoma. Although the presence of private mutations was observed in all analyzed tumors, there was no evidence of subclonality of cancer driver genes in the other patients.

It is well established that most somatic mutations acquired in melanomas are C>T transitions preceded by a pyrimidine representing UVB-induced mutations. We found that approximately 80% of all trunk mutations harbored the UVB signature, while there was a span of 20%–70% of branch mutations having the UVB signature (Fig. 3; $P < 0.001$). On the other hand, T>G transversions characteristic of UVA mutation signature (28) were significantly increased among the branch mutations as compared with trunk mutations ($P < 0.001$, Fisher exact test). These findings indicate that different mutational processes are operative during the progression of melanoma (Supplementary Fig. S9). Notably, the only case biopsied during treatment (Mm1742) did not show a decrease of UVB- or increase of UVA-induced mutations (Fig. 3).

Finally, we constructed phylogenetic trees for these tumors by maximum parsimony analysis (Fig. 4). We observed a branched evolutionary pattern in tumor Mm1641 where seven distinct regions were subjected to WES. In contrast, Mm1749 showed limited degree of branching, even though these were different in-transit metastases removed simultaneously. Inclusion of three additional asynchronous in-transit metastases

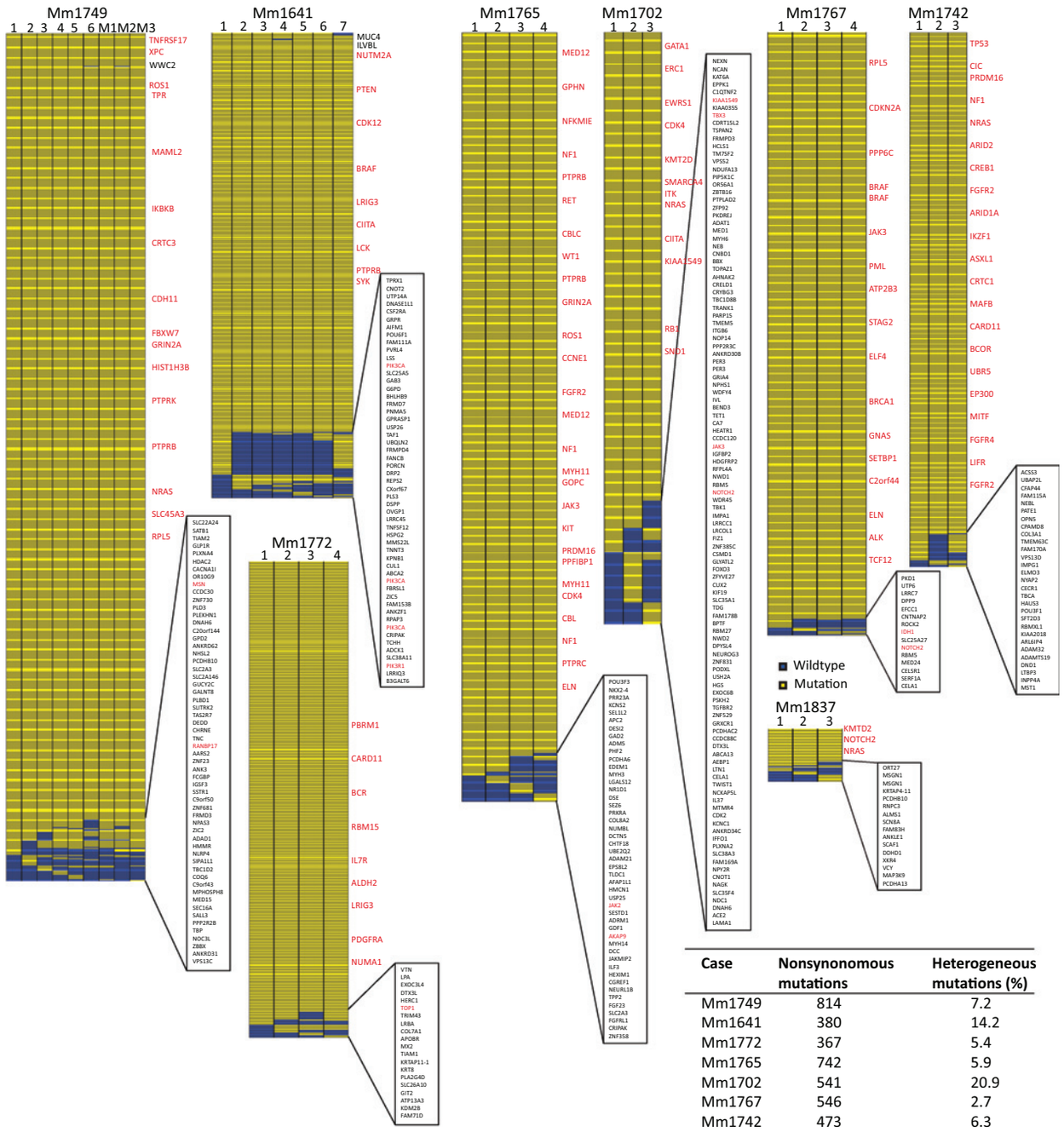

Case	Nonsynonomous mutations	Heterogeneous mutations (%)
Mm1749	814	7.2
Mm1641	380	14.2
Mm1772	367	5.4
Mm1765	742	5.9
Mm1702	541	20.9
Mm1767	546	2.7
Mm1742	473	6.3
Mm1837	45	37.8

Figure 1.
Regional distribution of mutations found in multitumor regions of eight melanoma patients. Presence (yellow) or absence (blue) of each mutation is marked for each tumor region. Insets provide gene symbols for the heterogeneous mutations in each case. Cancer Gene Census genes are marked in red. The table shows numbers of nonsynonymous mutations and percentage of heterogeneous mutations in each case. Notably, for Mm1742, the melanoma metastasis was removed during temozolomide treatment.

supported the limited branched evolution in Mm1749. In the phylogenetic tree it is clearly observed that M1-3 is closely intermingled with R1-6. In conclusion, the branched evolutionary pattern indicates that a linear progression model does not sufficiently explain melanoma evolution.

Transcriptome analysis of intratumor heterogeneity

We then performed microarray-based gene expression profiling of all samples to determine the transcriptional heterogeneity within individual tumors. Importantly, we pooled the data from the multiregion samples with a reference set of 214 metastatic

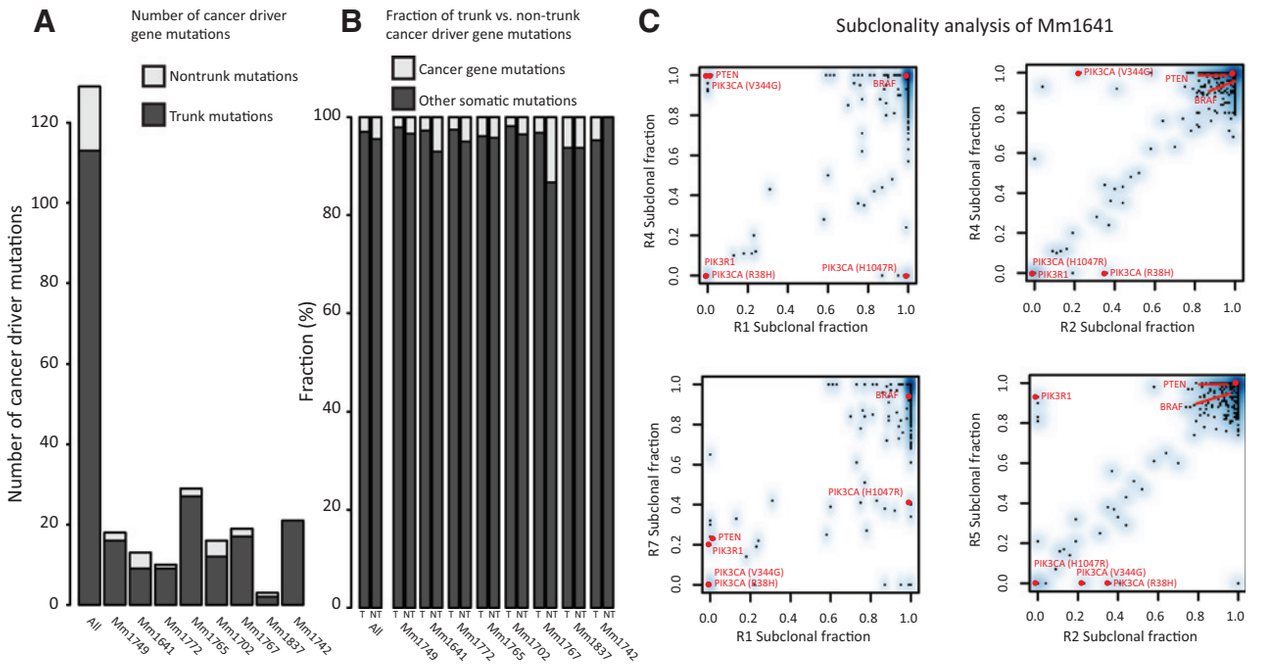

Figure 2.

Analysis of cancer gene mutations and subclonality in melanoma tumors. **A,** bar plot displaying the number of mutations in cancer census genes ($n = 129$). Mutations are divided in trunk (T, shared mutations present in all regions) and nontrunk (NT, mutations not present in all regions). **B,** fractions of cancer gene mutations among trunk (T) and nontrunk (NT) mutations demonstrating that only a fraction of all T and NT mutations are alterations in cancer driver genes. **C,** mutation plot demonstrating the subclonality analysis in different regions of tumor Mm1641 that displayed the most distinct subclonal pattern. The subclonal fraction is obtained from the ABSOLUTE analysis. Subclonal fractions of all mutations in two regions are plotted on the *x*- and *y*-axis. Melanoma driver mutations such as BRAF mutations and mutations in the PI3K pathway are indicated in the plots.

melanoma tumors previously profiled using the same platform, allowing to relate the gene expression levels of the ITH regions in relation to the full melanoma expression space (22). We determined the intratumoral expression of a subtype signature shown to classify melanomas into four molecular subgroups: high-immune (associated with a good prognosis), microphthalmia-associated transcription factor (MITF)-low proliferative (associated with a poor prognosis), MITF-high pigmentation (associated with a poor prognosis), and normal-like. In 4 of 8 patients, we could observe gene expression–based ITH when taking into account genes that have been used to develop the subtype classification. Inconsistent with the phylogenetic tree analysis, we observed that two regions evolutionary similar by mutation analysis could be assigned to different gene expression subtypes (Fig. 5). For example, based on phylogenetic tree analysis in Mm1641, R1, and R7 displayed genetic divergence. However, based on gene expression subtype analysis, R3 and R5 demonstrated different gene expression classification. Such differences were also observed patients Mm1702, Mm1749, and Mm1742.

Next, we investigated mRNA levels of 10 genes involved in melanocyte differentiation (*MITF*, *MLANA*, *TYR*), immune checkpoint (*CTLA4*, *PD1*), T-cell functions (*CD3*, *CD247*, *CD8A*), and cell proliferation (*CCNE1*, *AURKA*; Fig. 5). *MITF* and its target genes (*MLANA* and *TYR*) displayed intratumor gene expression differences and showed agreement with the subtype classification. Furthermore, mRNA levels of immune checkpoint genes (*CTLA4* and *PD1*) showed some consistency with the phylogenetic tree analysis. For example, R1 and R2 from Mm1765 had decreased levels of *CTLA4* and these two regions formed a distinct branch that seemed to have evolved later than R3 and R4, suggesting that some clones may evolve to escape the immune response (Figs. 3 and 5). Gene copy number values extracted from the WES data were used to determine an additional layer of ITH and unveiled additional information using GISTIC regions from the melanoma Cancer Genome Atlas study (24). The amount of copy number changes per tumor varied between patients. For example, Mm1765 harbored copy number changes exclusively on chromosomes 1q, 6p24.3, and 9p23 with a heterogeneous pattern at chromosome 9p23 (Fig. 5). In Mm1749, several copy number changes were identified with three in-transit metastases lacking a *CDKN2A* homozygous deletion detected in all the other six metastases. Mm1837 harbored the highest degree of mutational ITH; however, we found no gene copy number differences. Overall, this suggests that ITH may independently be dictated by mutations, DNA copy number changes, or gene expression.

RNA-seq reveals allele-specific expression

Finally, we performed RNA sequencing to determine spatially restricted mutation allele–specific expression. The majority of mutated genes had low or absent expression, as only about 40% of mutated genes were expressed and <20% had >20 reads (Fig. 6A). To determine allele-specific expression, we used the >20 read cutoff to obtain robust frequencies of the mutated allele, and correlated the variant allele frequency (VAF) of the RNA to the VAF of the DNA. In line with Castle and colleagues (29), we observed a good correlation between RNA and DNA VAF for the majority of

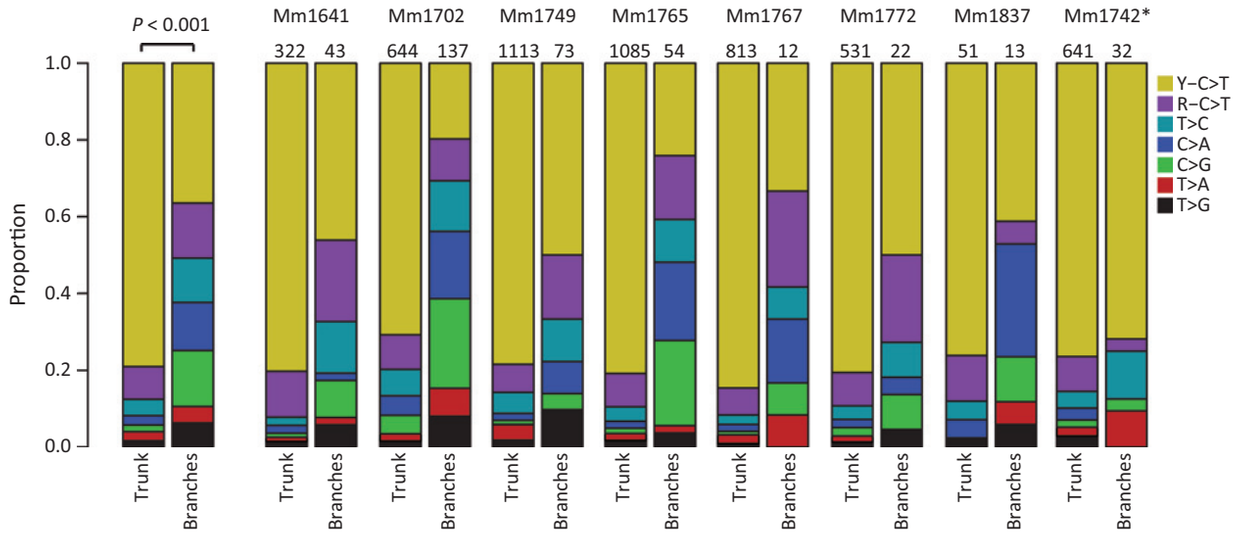

Figure 3.

Mutational signatures in melanoma revealed by multiregion sequencing. Fraction of each kind of base substitution is shown for trunk (shared) and branch (heterogeneous) SNVs for each patient. The two left columns represent mutations combined from all patients. A Fisher exact test was used to determine differences in mutational spectrum between trunk and branch mutations. Color codes reflect the different base substitutions, with C>T mutations divided into two groups: Y-C>T denotes C-to-T mutations at sites preceded by a pyrimidine (Y), and R-C>T denotes those preceded by a purine (R). *, the patient treated with temozolomide at the time of surgery.

mutations, that is, the mutated allele was expressed according to its frequency in the DNA (Fig. 6B). As an exception from this rule and in accordance with the concept of nonsense-mediated mRNA decay, we found that alleles harboring stop mutations had significantly lower expression as compared with alleles harboring synonymous or missense mutations (Fig. 6C). As expected, a significant fraction of genes with mutations at chromosomal loci undergoing loss of heterozygosity (LOH) demonstrated preferential expression of the mutated allele. Subsequently, we used a binomial test to identify genes with preferential expression of the mutated allele and identified a limited number of genes. Only *TNC* had a branch mutation with preferential expression of the mutated allele in three different in-transit metastases from patient Mm1749. The vast majority of the genes harboring nontrunk mutations were expressed at similar mRNA levels in tumor regions with and without the mutation (Supplementary Fig. S10). We found several genes with trunk mutations, however, with a preferential expression of mutated allele in only one of the spatially separated regions. For example, Mm1765 harbored a *KIT* D816V mutation found at equal DNA allele frequencies in all spatially separated regions, with preferential overexpression of the mutated allele only in R3 (Fig. 6D and Supplementary Figs. S11–S15). Collectively, our data suggest that preferential expression of the mutated allele occurs; however, it does not seem to be a general mechanism of melanomagenesis.

Discussion

We have identified ITH of somatic mutations, DNA copy number, and transcriptomic changes in multiple regions from eight melanoma tumors and demonstrated that 3%–38% of somatic mutations were not identified in all regions of the tumors. In contrast to renal cell cancer, where approximately 75% of cancer driver mutations are affected by ITH (2), we found only 12% of cancer driver mutations to be affected by ITH, indicating that heterogeneous mutations were predominantly passenger mutations. Moreover, ITH seemed to be independent of the number of biopsies analyzed, as the tumor with only three regions analyzed showed the highest degree of ITH, suggesting that the degree of ITH could vary in melanoma.

In line with other melanoma sequencing studies (9, 30), we detected UVB-induced C>T transitions. Our analysis confirms that this signature is enriched early in melanoma tumor evolution occurring in all tumor regions. We found a significant reduction of the UVB-induced mutational signature in branch (nontrunk) mutations, suggesting that mutations arising later in the progression of melanoma may occur as a result of other mutational processes. This is in line with recent studies in lung cancer, where later acquired mutations lack the tobacco-smoking signature (3, 4). Furthermore, with the exception of one patient in current study none received any systemic treatment prior to surgical removal of tumor; therefore, the switch in mutational processes is likely due to evolutionary changes occurring during melanoma progression and not due to extrinsic factors. This further highlights the benefit of multiregion sequencing as different mutational processes operate during tumor evolution.

We confirmed previous findings consistent with activating somatic mutations in the MAPK pathway being driver events in the majority of melanomas (24). We showed that constitutive activation of *BRAF*, *KIT*, and *NRAS* through somatic mutations was ubiquitous in seven patients. The last patient was wild-type for *BRAF*, *NRAS*, *NF1*, and *KIT*; however, the tumor harbored a nonkinase domain *PDGFRA* mutation. In contrast, we found evidence of genetic mutations in the PI3K pathway occurring as nontrunk events. In particular, we found parallel evolution of three distinct activating *PIK3CA* mutations (p.V344G, p.R38H, and p.H1047R) and a stop mutation in *PIK3R1* in a large lymph node metastasis (Mm1641). Mutational convergence affecting

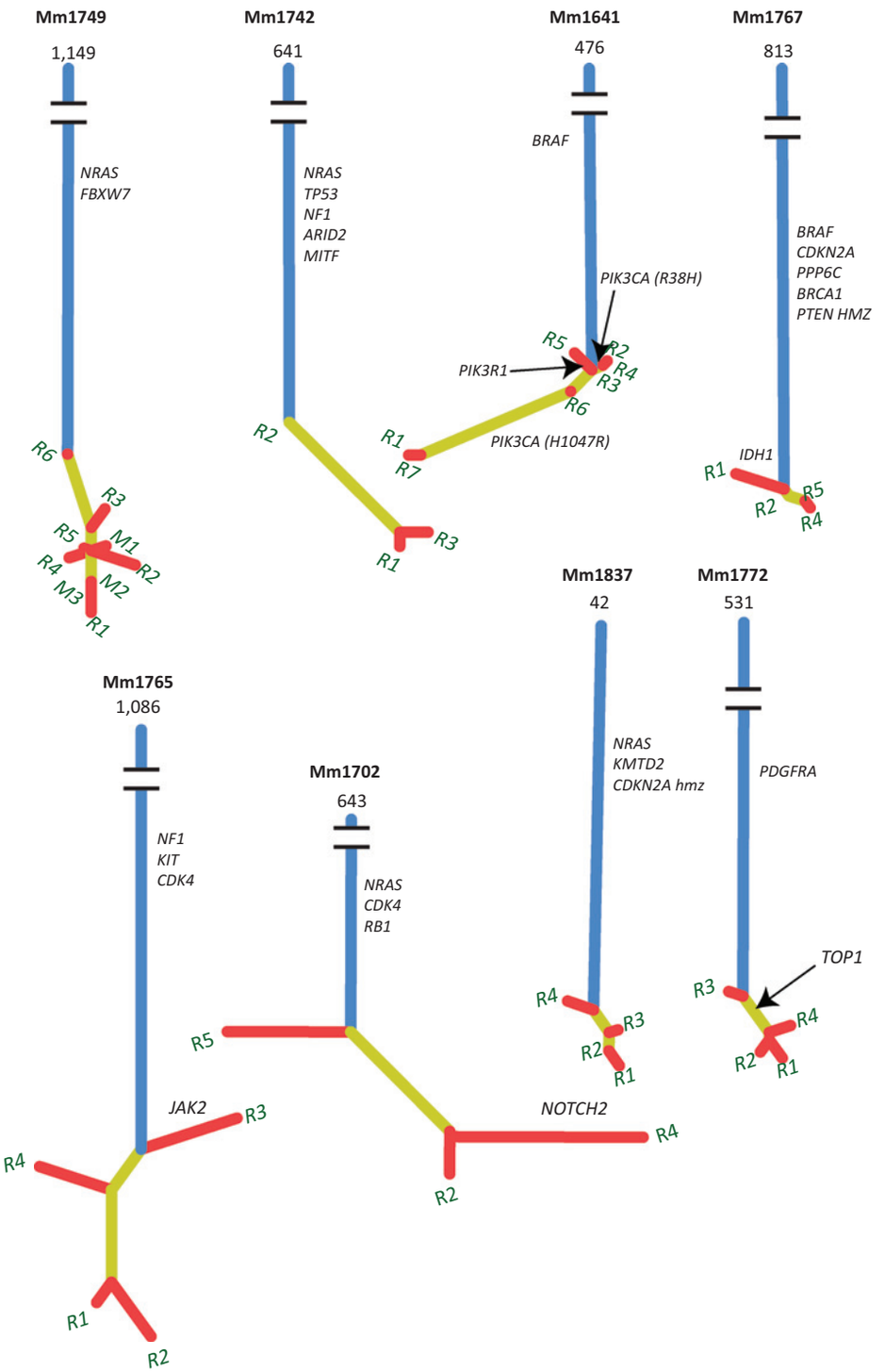

Figure 4.
Phylogenetic trees of mutation evolution from different regions of eight melanoma patients generated by maximum parsimony analysis from exome data. The number of somatic mutations common to all tumor regions is indicated at the top of each tree. The different tumor regions (R) are indicated at the ends of the branches. In case Mm1749, M1-3 represent three asynchronous in-transit metastases. Length of branch reflects number of mutations. Blue, the stem of the tree with all shared mutations; yellow, branches shared by at least two regions; red branch, individual regions. Also indicated in the phylogenetic tree are mutations in melanoma cancer driver genes.

different PI3K members in single melanoma tumors implicate that activation of this pathway is involved in later stages of metastatic melanoma progression. In addition, activation of the PI3K pathway via somatic mutations may be a reason for acquired resistance to BRAF inhibition as previously described (31). Indeed, patient Mm1641 received BRAF inhibition after surgery but subsequently developed resistance to the therapy.

Although it is difficult to discern the full extent of ITH at all levels using multiregion sequencing only, we observed that patients having melanoma tumors with high degree of ITH as revealed by our approach experienced a more aggressive disease course. These findings are further supported by data from similar studies in lung cancer, esophageal adenocarcinoma, and pediatric tumors (4, 8, 32). However, given that this study included a

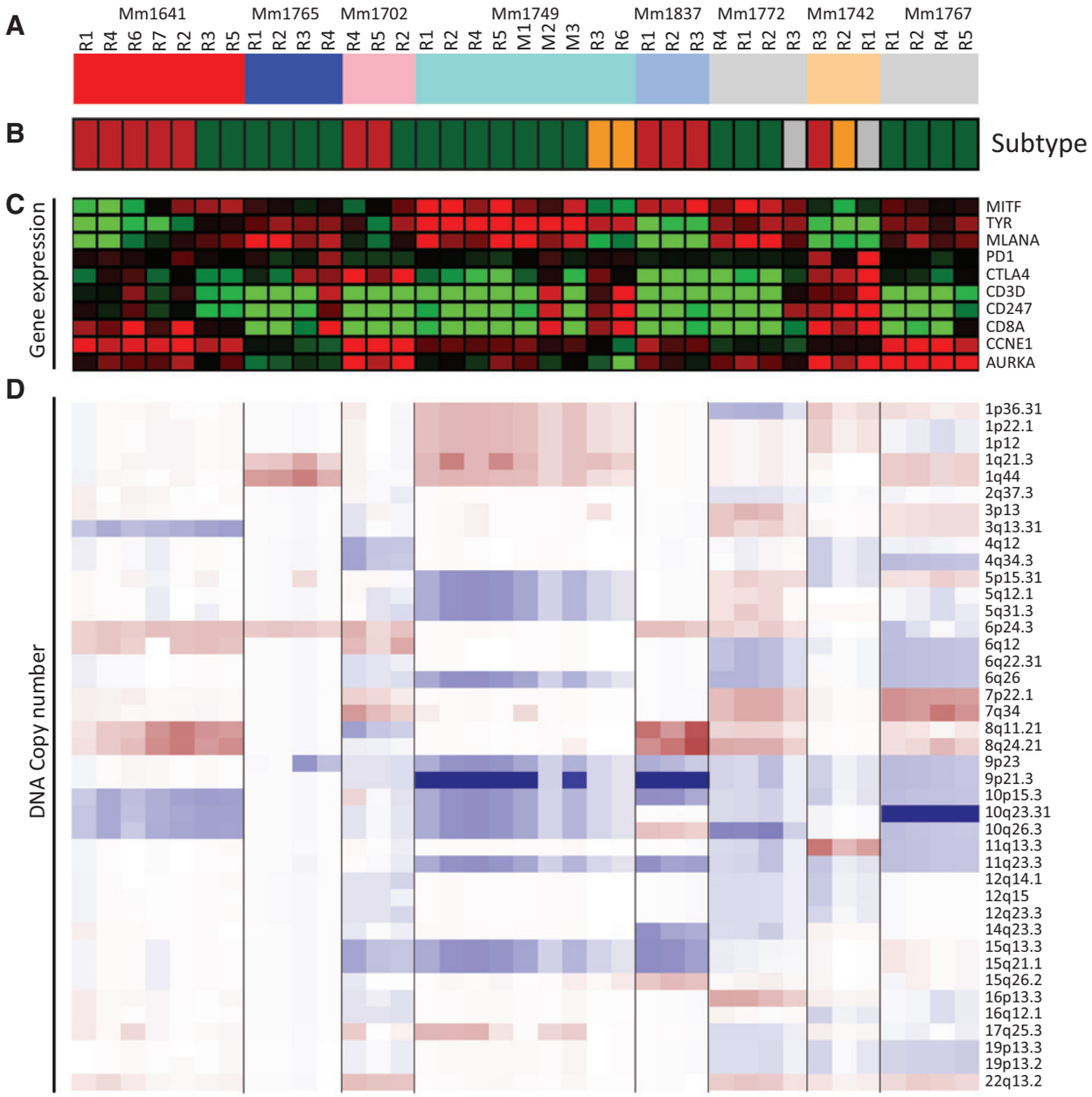

Figure 5.

Gene expression and DNA copy number aberrations analysis for the eight melanoma patients. For each tumor site/patient (**A**), the following information is shown (panels from top): **B,** molecular subtype [high-immune (orange), pigmentation (green), proliferative (red), normal-like (blue), and unclassified (gray; ref. 22). **C,** expression of pigmentation, immune response, and proliferation genes (green, downregulation; red, upregulation). **D,** copy number levels of GISTIC regions defined by the The Cancer Genome Atlas melanoma study (24). For copy number aberrations, blue denotes loss of genetic material and red denotes gain thereof.

limited number of patients all treated differently, additional larger studies are required to further confirm these data given the significance of prognostic markers in melanoma.

Addressing an additional layer of genomic heterogeneity we investigated the expression of mutated alleles using RNA sequencing. In line with the results of Castle and colleagues (29), we found a good correlation (corr. = 0.57) between DNA and RNA VAFs. Our molecular exploration of ITH in melanoma further showed that there is considerable variation in prognostic gene expression signatures within individual melanoma tumors in line with results from studies in renal cell cancer (2). However, the analyzed gene signatures are partly dependent on the tumor microenvironment, highlighting another layer of genomic complexity within melanoma tumors.

Taken together, we have used a multiregion sequencing approach in early-stage treatment-naïve metastatic melanomas

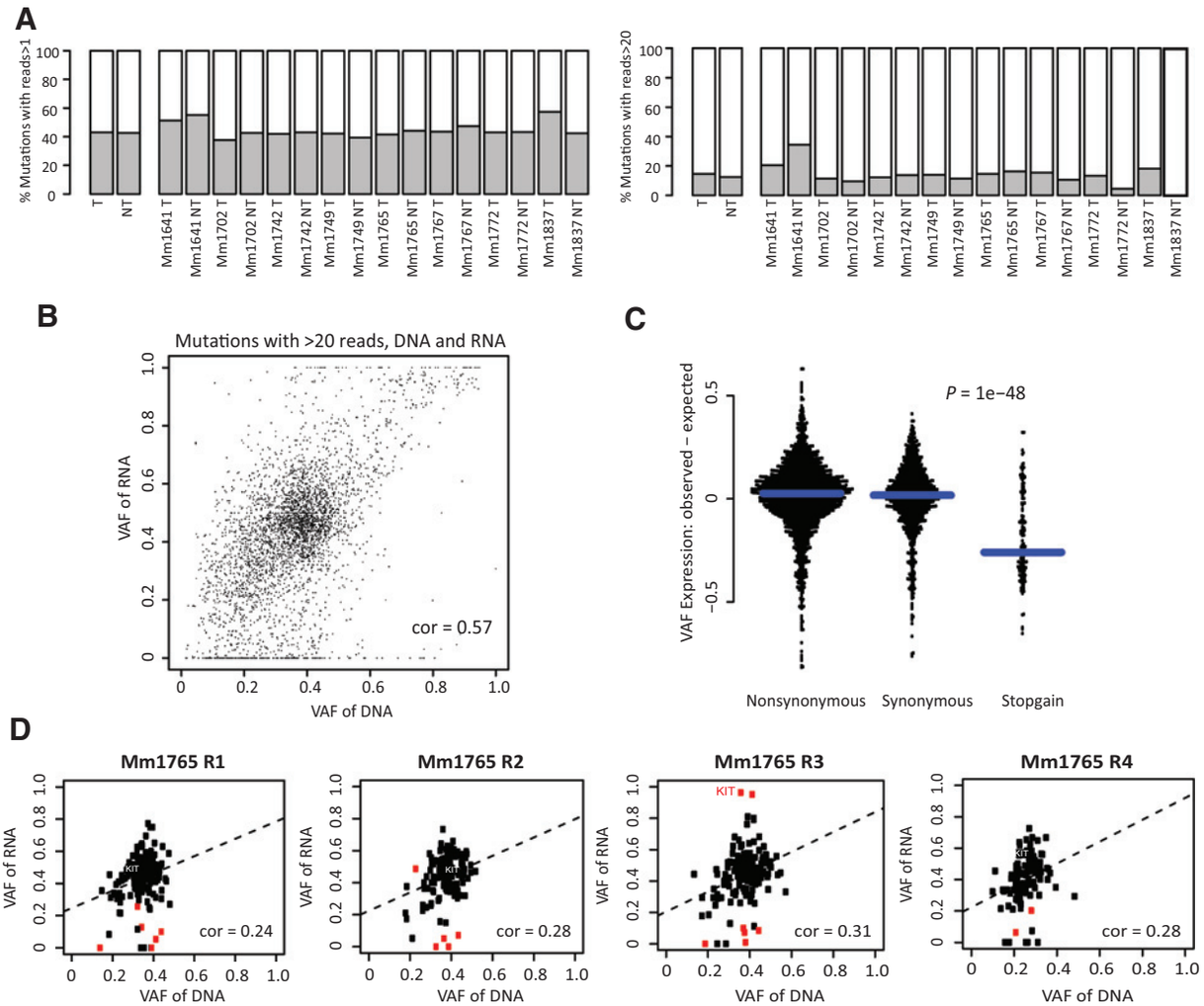

Figure 6.

RNA sequencing of melanoma samples from eight patients. **A,** fraction of all mutations present in >1 read (left) and >20 reads (right). **B,** correlation plot between DNA and RNA VAF across all samples. **C,** analysis of VAF expression versus expected expression for synonymous, nonsynonymous, and stop mutations in all samples. **D,** correlation plots in individual regions in Mm1765, which was the only sample displaying preferential expression of a cancer driver gene. Preferential expression of the KIT mutated allele observed only in R3 is indicated in the plots. Red, significant values using a binomial test as described in Supplemental information. Cor., Spearman correlation value between DNA and RNA VAF.

and showed that ITH was directed by either mutational or gene expression heterogeneity, suggesting a dual layer of genomic complexity in the heterogeneity of melanoma tumors. This study represents the first comprehensive genomic investigation of intratumor heterogeneity in metastatic melanoma and complements the findings by Shain and colleagues on genetic evolution of melanoma from precursor lesions (33). Although the majority of mutations in cancer driver genes such as *BRAF*V600E occurred ubiquitously throughout the tumor, mutations in the PI3K pathway demonstrated a heterogeneous pattern, suggesting that genetic events occurring in this pathway represent later acquired mutations in metastatic melanoma evolution. Furthermore, Shain and colleagues (33) found that UVB is the main factor in both the initiation of precursor lesions and their progression to primary melanoma; however, our results implicate that there are other mutational processes operating during the evolution of metastatic melanoma. Thus, early melanoma progression may be dependent on UVB-induced mutagenesis, while later metastatic evolution is associated with additional non-UVB mutational processes. Importantly, our results further indicate that mutation based ITH may be a prognostic biomarker, as patients with high degree of mutational heterogeneity presented with an aggressive disease course. Extension of research to epigenetic and clinical assessment in much larger cohorts, preferably with repeated biopsies at relapse after treatment, is needed to fully understand the clinical and biologic impact of ITH in melanoma.

Disclosure of Potential Conflicts of Interest

No potential conflicts of interest were disclosed.

Authors' Contributions

Conception and design: K. Harbst, A. Borg, C. Ingvar, A. Carneiro, G. Jonsson

Development of methodology: K. Harbst, M. Lauss, G. Jonsson

Acquisition of data (provided animals, acquired and managed patients, provided facilities, etc.): K. Harbst, K. Isaksson, F. Rosengren, T. Törngren, M.C. Johansson, B. Baldetorp, A. Borg, C. Ingvar, A. Carneiro, G. Jonsson

Analysis and interpretation of data (e.g., statistical analysis, biostatistics, computational analysis): K. Harbst, M. Lauss, H. Cirenajwis, A. Kvist, J. Vallon-Christersson, B. Baldetorp, H. Olsson, A. Carneiro, G. Jonsson

Writing, review, and/or revision of the manuscript: K. Harbst, M. Lauss, H. Cirenajwis, K. Isaksson, J. Vallon-Christersson, H. Olsson, C. Ingvar, A. Carneiro, G. Jonsson

Administrative, technical, or material support (i.e., reporting or organizing data, constructing databases): A. Carneiro, G. Jonsson

Study supervision: K. Harbst, C. Ingvar, A. Carneiro, G. Jonsson

Grant Support

The Swedish Research Council, the Swedish Cancer Society, the Berta Kamprad Foundation, The Gunnar Nilsson Cancer foundation, the Gustav Vth Jubilee Foundation, and Governmental Funding of Clinical Research within National Health Service.

The costs of publication of this article were defrayed in part by the payment of page charges. This article must therefore be hereby marked *advertisement* in accordance with 18 U.S.C. Section 1734 solely to indicate this fact.

Received January 3, 2016; revised March 10, 2016; accepted March 28, 2016; published OnlineFirst May 23, 2016.

References

1. Gerlinger M, Rowan AJ, Horswell S, Larkin J, Endesfelder D, Gronroos E, et al. Intratumor heterogeneity and branched evolution revealed by multiregion sequencing. N Engl J Med 2012;366:883–92.
2. Gerlinger M, Horswell S, Larkin J, Rowan AJ, Salm MP, Varela I, et al. Genomic architecture and evolution of clear cell renal cell carcinomas defined by multiregion sequencing. Nat Genet 2014;46:225–33.
3. de Bruin EC, McGranahan N, Mitter R, Salm M, Wedge DC, Yates L, et al. Spatial and temporal diversity in genomic instability processes defines lung cancer evolution. Science 2014;346:251–6.
4. Zhang J, Fujimoto J, Zhang J, Wedge DC, Song X, Zhang J, et al. Intratumor heterogeneity in localized lung adenocarcinomas delineated by multiregion sequencing. Science 2014;346:256–9.
5. Bashashati A, Ha G, Tone A, Ding J, Prentice LM, Roth A, et al. Distinct evolutionary trajectories of primary high-grade serous ovarian cancers revealed through spatial mutational profiling. J Pathol 2013;231:21–34.
6. Boutros PC, Fraser M, Harding NJ, de Borja R, Trudel D, Lalonde E, et al. Spatial genomic heterogeneity within localized, multifocal prostate cancer. Nat Genet 2015;47:736–45.
7. Cooper CS, Eeles R, Wedge DC, Van Loo P, Gundem G, Alexandrov LB, et al. Analysis of the genetic phylogeny of multifocal prostate cancer identifies multiple independent clonal expansions in neoplastic and morphologically normal prostate tissue. Nat Genet 2015;47:367–72.
8. Murugaesu N, Wilson GA, Birkbak NJ, Watkins TB, McGranahan N, Kumar S, et al. Tracking the genomic evolution of esophageal adenocarcinoma through neoadjuvant chemotherapy. Cancer Discov 2015;5:821–31.
9. Alexandrov LB, Nik-Zainal S, Wedge DC, Aparicio SA, Behjati S, Biankin AV, et al. Signatures of mutational processes in human cancer. Nature 2013;500:415–21.
10. Harbst K, Lauss M, Cirenajwis H, Winter C, Howlin J, Torngren T, et al. Molecular and genetic diversity in the metastatic process of melanoma. J Pathol 2014;233:39–50.
11. Sanborn JZ, Chung J, Purdom E, Wang NJ, Kakavand H, Wilmott JS, et al. Phylogenetic analyses of melanoma reveal complex patterns of metastatic dissemination. Proc Natl Acad Sci U S A 2015;112:10995–1000.
12. Chapman PB, Hauschild A, Robert C, Haanen JB, Ascierto P, Larkin J, et al. Improved survival with vemurafenib in melanoma with BRAF V600E mutation. N Engl J Med 2011;364:2507–16.
13. Landau DA, Carter SL, Stojanov P, McKenna A, Stevenson K, Lawrence MS, et al. Evolution and impact of subclonal mutations in chronic lymphocytic leukemia. Cell 2013;152:714–26.
14. Mroz EA, Rocco JW. MATH, a novel measure of intratumor genetic heterogeneity, is high in poor-outcome classes of head and neck squamous cell carcinoma. Oral Oncol 2013;49:211–5.
15. Kemper K, Krijgsman O, Cornelissen-Steijger P, Shahrabi A, Weeber F, Song JY, et al. Intra- and inter-tumor heterogeneity in a vemurafenib-resistant melanoma patient and derived xenografts. EMBO Mol Med 2015;7:1104–18.
16. Cibulskis K, Lawrence MS, Carter SL, Sivachenko A, Jaffe D, Sougnez C, et al. Sensitive detection of somatic point mutations in impure and heterogeneous cancer samples. Nat Biotechnol 2013;31:213–9.
17. Koboldt DC, Zhang Q, Larson DE, Shen D, McLellan MD, Lin L, et al. VarScan 2: somatic mutation and copy number alteration discovery in cancer by exome sequencing. Genome Res 2012;22:568–76.
18. Wang K, Li M, Hakonarson H. ANNOVAR: functional annotation of genetic variants from high-throughput sequencing data. Nucleic Acids Res 2010;38:e164.
19. Li J, Lupat R, Amarasinghe KC, Thompson ER, Doyle MA, Ryland GL, et al. CONTRA: copy number analysis for targeted resequencing. Bioinformatics 2012;28:1307–13.
20. Hupe P, Stransky N, Thiery JP, Radvanyi F, Barillot E. Analysis of array CGH data: from signal ratio to gain and loss of DNA regions. Bioinformatics 2004;20:3413–22.
21. Carter SL, Cibulskis K, Helman E, McKenna A, Shen H, Zack T, et al. Absolute quantification of somatic DNA alterations in human cancer. Nat Biotechnol 2012;30:413–21.
22. Cirenajwis H, Ekedahl H, Lauss M, Harbst K, Carneiro A, Enoksson J, et al. Molecular stratification of metastatic melanoma using gene expression profiling: Prediction of survival outcome and benefit from molecular targeted therapy. Oncotarget 2015;6:12297–309.
23. Saal LH, Vallon-Christersson J, Hakkinen J, Hegardt C, Grabau D, Winter C, et al. The Sweden Cancerome Analysis Network - Breast (SCAN-B) Initiative: a large-scale multicenter infrastructure towards implementation of breast cancer genomic analyses in the clinical routine. Genome Med 2015;7:20.
24. The Cancer Genome Atlas Network. Genomic classification of cutaneous melanoma. Cell 2015;161:1681–96.
25. Curtin JA, Busam K, Pinkel D, Bastian BC. Somatic activation of KIT in distinct subtypes of melanoma. J Clin Oncol 2006;24:4340–6.
26. Futreal PA, Coin L, Marshall M, Down T, Hubbard T, Wooster R, et al. A census of human cancer genes. Nat Rev Cancer 2004;4:177–83.
27. Saal LH, Holm K, Maurer M, Memeo L, Su T, Wang X, et al. PIK3CA mutations correlate with hormone receptors, node metastasis, and ERBB2, and are mutually exclusive with PTEN loss in human breast carcinoma. Cancer Res 2005;65:2554–9.
28. Drobetsky EA, Turcotte J, Chateauneuf A. A role for ultraviolet A in solar mutagenesis. Proc Natl Acad Sci U S A 1995;92:2350–4.
29. Castle JC, Loewer M, Boegel S, Tadmor AD, Boisguerin V, de Graaf J, et al. Mutated tumor alleles are expressed according to their DNA frequency. Sci Rep 2014;4:4743.
30. Hodis E, Watson IR, Kryukov GV, Arold ST, Imielinski M, Theurillat JP, et al. A landscape of driver mutations in melanoma. Cell 2012;150:251–63.
31. Haarberg HE, Smalley KS. Resistance to Raf inhibition in cancer. Drug Discov Today Technol 2014;11:27–32.
32. Mengelbier LH, Karlsson J, Lindgren D, Valind A, Lilljebjorn H, Jansson C, et al. Intratumoral genome diversity parallels progression and predicts outcome in pediatric cancer. Nat Commun 2015;6:6125.
33. Shain AH, Yeh I, Kovalyshyn I, Sriharan A, Talevich E, Gagnon A, et al. The genetic evolution of melanoma from precursor lesions. N Engl J Med 2015;373:1926–36.